



HAL
open science

Direct Numerical Simulation of polydisperse evaporating sprays in 3D jet configuration using Euler-Euler and Euler-Lagrange formalisms

L Fréret, O Thomine, F Laurent, J Réveillon, M Massot

► To cite this version:

L Fréret, O Thomine, F Laurent, J Réveillon, M Massot. Direct Numerical Simulation of polydisperse evaporating sprays in 3D jet configuration using Euler-Euler and Euler-Lagrange formalisms. Center for Turbulence Research Proceedings of the Summer Program 2012, pp.345-354, 2012. hal-03105827

HAL Id: hal-03105827

<https://hal.science/hal-03105827>

Submitted on 29 Jan 2021

HAL is a multi-disciplinary open access archive for the deposit and dissemination of scientific research documents, whether they are published or not. The documents may come from teaching and research institutions in France or abroad, or from public or private research centers.

L'archive ouverte pluridisciplinaire **HAL**, est destinée au dépôt et à la diffusion de documents scientifiques de niveau recherche, publiés ou non, émanant des établissements d'enseignement et de recherche français ou étrangers, des laboratoires publics ou privés.

Direct Numerical Simulation of polydisperse evaporating sprays in 3D jet configuration using Euler-Euler and Euler-Lagrange formalisms

By L. Fréret[†], O. Thomine[‡], F. Laurent[¶], J. Réveillon^{||} AND M. Massot[¶]

The use of robust and accurate Eulerian/Eulerian formulations in the modeling of reactive two-phase flow would be a major step forward in the framework of turbulent combustion modeling with massively parallel supercomputers. In the present contribution we rely on the recent developments conducted in the framework of homogeneous isotropic turbulence (Fréret *et al.* 2010; Fréret *et al.* 2012) using the Eulerian multi-fluid model (MF) in the context of Direct Numerical Simulation (DNS) to capture all stages of turbulent spray combustion for polydisperse sprays, and set up a 3D free jet configuration, thus reaching the next step of turbulent shear flows. The robustness and accuracy of the model and related numerical methods are evaluated and assessed on two configurations with non-evaporating and evaporating spray injection. With MF, we obtain the same level of accuracy as a baseline solution obtained with Lagrangian droplet tracking for rather similar computational time on a few hundred processors. This study yields a solid premise for the future 3D reacting configurations.

1. Introduction

Spray combustion modeling is a fundamental stage in the design of combustion chambers that relies on accurate computational tools to rapidly design and develop high efficiency, low emission engines. Once the atomization processes have lead to a polydisperse spray carried by a turbulent gaseous flow field, many different time and space characteristic scales, especially during evaporation and combustion, have to be modeled and resolved. Thus, such two-phase flow models need dedicated models and numerical methods in order to characterize correctly complex industrial flows in CFD solvers. In such configurations, the gas, which is a continuum, is best represented by a Eulerian description. However, in the framework of disperse flows, particles or droplets can be modeled either by discrete particle simulations or by a statistical approach through a Williams-Boltzmann equation. The latter model can be discretized either through a Lagrangian or a Eulerian description (de Chaisemartin 2009; Fréret *et al.* 2012). Both descriptions are now well established and they have proven their efficiency in multi-phase flow simulations. Lagrangian methods combine an efficient modeling of the polydisperse phase as well as an easiness of implementation. Nevertheless, in the framework of 3D simulations, with unsteady configurations and polydisperse sprays, massively parallel computations require the use of complex and costly dynamic partitioning methods, to ensure a good load balancing between the different parallel processes (see Garcia 2009) and lead to

[†] Laboratoire d'Imagerie Paramétrique, 15 rue de l'école de médecine, 75006 Paris, France

[‡] Institut de Recherche sur la Fusion Magnétique, CEA Cadarache, 13108 St Paul Les Durance

[¶] Laboratoire EM2C - UPR CNRS 288, Ecole Centrale Paris, 92295 Chatenay Malabry Cedex

^{||} CORIA, UMR 6614, Avenue de l'université, 76800 St-Etienne du Rouvray, France

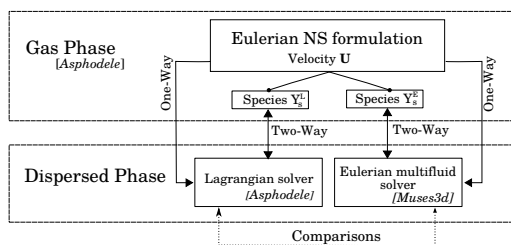


FIGURE 1. Sketch of the coupling between Eulerian and Lagrangian codes. *Muses3d* is a Eulerian solver for the dispersed phase while *Asphodele* is a Lagrangian solver for the dispersed phase and a Eulerian solver for the gas phase.

difficulties in order to reach some level of convergence and a limited level of noise with reasonable computational cost. Hence, Eulerian methods provide a very interesting alternative to Lagrangian methods, since they can easily take advantage of massively parallel computations with a high level of efficiency as proven in Fréret *et al.* (2010); Fréret *et al.* (2012). Eulerian methods however require special attention in terms of modeling, mathematical structure and dedicated numerical methods in order to properly control numerical diffusion (Massot *et al.* 2009; de Chaisemartin *et al.* 2009; Fréret *et al.* 2012).

In the present contribution, we will focus on the DNS of polydisperse sprays in turbulent flow field with sufficiently small inertia so that a monokinetic assumption introduced in Laurent & Massot (2001) remains valid (for a discussion about droplet trajectory crossing, we refer to Kah *et al.* (2010); Vié *et al.* (2012); Doisneau *et al.* (2012)). Recent results initiated during the Summer Program 2010 (Fréret *et al.* 2010; Fréret *et al.* 2012) in the framework of homogeneous isotropic turbulence have shown the potential of such methods in order to reproduce accurately and efficiently the propagation of a flame in a polydisperse evaporating spray compared to an Eulerian-Lagrangian (EL) approach. The objective of the present work is to investigate the extension of such a comparison in the framework of turbulent shear flows and to carry out the first exhaustive comparisons between Eulerian-Lagrangian (EL) and Eulerian-Eulerian (EE) formulations of a turbulent 3D round jet with non-evaporating and evaporating polydisperse sprays.

2. Two-phase flow simulations

2.1. Gas and disperse phase models and numerical methods

We study the coupling of the Navier-Stokes-Fourier equations under the Low-Mach number limit with, on the one side, a set of discrete particles for the EL model, and on the other side, with the MF derived from the Williams-Boltzmann equation (Massot *et al.* 2009; Fréret *et al.* 2012). The EL spray description requires the resolution of a large number of ODEs, which is governing the dynamics of the spray in physical and phase space, whereas the MF requires the resolution of several sets of conservation equations using finite volume methods on structured grids. One of the key issues of our study relies on the fact that we will compare both approaches by coupling each of them with the same gaseous flow field resolved in time in order to properly assess the methods and their ability to resolve the details of the dynamics. We thus use a one-way coupling as far as momentum and heat transfers are concerned. In order to capture evaporation and mass transfer and potentially saturation effects, we use a two-way coupling in terms of mass transfer, with the proper assumption in order not to impact the gaseous flow field. Indeed, the evaporated fuel is not added as a mass source term in the gaseous

equations, but is stored in two passive scalars, one for each description of the spray, that are transported by the flow. Consequently, two sets of species mass fractions are resolved and transported by a single gaseous flow field, each of them being coupled to the Lagrangian/Eulerian spray resolution. The Lagrangian gaseous fuel mass fraction is obtained through a projection of the droplet evaporation over the neighbor cells of the gaseous mesh. The gaseous flow field is resolved using the *Asphodele* code developed at CORIA in the group of J. Reveillon. This code also resolves the Lagrangian description of the spray and it is coupled to the *Muses3d* code developed at EM2C Lab in the group of M. Massot in order to solve the MF. The strategy is summarized in Fig 1.

More specifically, the evolution of the air/vapor mixture is governed by a convection/diffusion equation with source terms coupled with either Lagrangian and Eulerian descriptions of the evaporating spray. The following relation applies for any species s , which stands for either the fuel (f), the oxidizer (o) or the burnt gases (b):

$$\frac{\partial Y_s^\alpha}{\partial t} + \frac{\partial Y_s^\alpha u_i}{\partial x_i} = D \frac{\partial^2 Y_s^\alpha}{\partial x_i^2} + \delta(s-f) \dot{d}_f^\alpha + \dot{\varepsilon}_s^\alpha, \quad (2.1)$$

where D is the species common diffusion coefficient and the velocity components u_i are obtained from the classical Navier-Stokes-Fourier equations in the Low Mach number limit (see Thomine 2011 for details in equations and numerical methods).

Two strictly independent sets of species equations are solved: Y_s^L that are coupled with the Lagrangian description of the spray and, on the other hand, Y_s^E that are coupled with the MF solver (see Fig 1). Only the velocity field evolution is common to both the mass fraction sets. Coupling each of the two dispersed phase solvers (Lagrangian and Eulerian) to the same gaseous phase dynamics is achieved through the mass source term \dot{d}_f^L and \dot{d}_f^E , respectively, with corrections $\dot{\varepsilon}_s^\alpha = -Y_s^\alpha \dot{d}_f^\alpha$ for each species involved in the description of the mixture. The correction allow to guarantee that the velocity field is not affected by the evaporation process and still remains the same for both methods. It guarantees that the sum of mass fractions remains equal to one at constant density.

As mentioned in the introduction, a discrete Lagrangian approach is adopted to follow the spray evolution within the gaseous oxidizer. By denoting a_k , \mathbf{v}_k and \mathbf{x}_k the diameter, the velocity and position vectors of every droplet k , respectively, the following relations:

$$\frac{d\mathbf{x}_k}{dt} = \mathbf{v}_k, \quad (2.2) \quad \frac{d\mathbf{v}_k}{dt} = \frac{(\mathbf{u}(\mathbf{x}_k, t) - \mathbf{v}_k)}{\beta_k^{(v)}}, \quad (2.3) \quad \frac{da_k^2}{dt} = -\frac{a_k^2}{\beta_k^{(a)}}, \quad (2.4)$$

are used to track the droplets throughout the computational domain. The vector \mathbf{u} represents the gas velocity at the droplet position \mathbf{x}_k . The right hand side term of equation (2.3) stands for a drag force applied to the droplet where $\beta_k^{(v)}$ is a dynamic relaxation time $\beta_k^{(v)} = \tau_p a_k^2 / a_0^2$. The diameter of the droplet k is a_k and a_0 is the initial diameter of any droplet of the initially monodisperse spray. The initial characteristic kinetic time of the considered droplets is denoted by τ_p . The unitary stoichiometric ratio leads to a global mass ratio of fuel of about 20%. The coefficient B is introduced in the expression of the evaporation rate through the evaporation time $\beta_k^{(a)}$ defined by $\beta_k^{(a)} = A a_k^2 / \ln(1+B)$. The coupling term $\dot{d}_f^{L(n)}$ affects the mixture fraction evolution owing to a distribution of the Lagrangian mass on the n^{th} node of the Eulerian grid. One may write $\dot{d}_f^{L(n)} = -\rho_d \frac{\pi}{4} \frac{1}{V} \sum_k \alpha_k^{(n)} a_k^3 / \beta_k^{(a)}$, where $\alpha_k^{(n)}$ is the distribution coefficient of the k^{th} droplet source term on the n^{th} node. Considering all the nodes affected by the k^{th} droplet, it is necessary to have $\sum_n \alpha_k^{(n)} = 1$ to conserve mass during the EL coupling.

The values of $\alpha_k^{(n)}$ are chosen as the regressive normalized distances between the droplets and all surrounding nodes.

For the Eulerian description of the spray, MF is used. It has been assessed for small and moderate Stokes numbers and can be derived from a kinetic level of description based on the monokinetic velocity distribution assumption conditioned on size (de Chaisemartin 2009). The droplet size phase space is then discretized into size intervals called sections and a system of conservation laws for each section $[S_k, S_{k+1}[$ is solved:

$$\begin{cases} \partial_t m^k + \partial_{\mathbf{x}} \cdot (m^k \mathbf{v}^k) = -(E_1^{(k)} + E_2^{(k)})m^k + E_1^{(k+1)}m^{(k+1)}, \\ \partial_t (m^k \mathbf{v}^k) + \partial_{\mathbf{x}} \cdot (m^k \mathbf{v}^k \otimes \mathbf{v}^k) = -(E_1^{(k)} + E_2^{(k)})m^k \mathbf{v}^k + E_1^{(k)}m^{(k+1)}\mathbf{v}^{(k+1)} + m^k \mathbf{F}^k, \\ \partial_t (m^k h^k) + \partial_{\mathbf{x}} \cdot (m^k h^k \otimes \mathbf{v}^k) = -(E_1^{(k)} + E_2^{(k)})m^k h^k + E_1^{(k)}m^{(k+1)}h^{(k+1)} + m^k C_{p,l} E_d^k, \end{cases}$$

where m^k is the mass concentration of droplets, \mathbf{v}^k and h^k are the average velocity and enthalpy in the k^{th} section, $C_{p,l}$ is the liquid heat capacity, $E_1^{(k)}$ are exchange terms between successive sections and $E_2^{(k)}$ are exchange terms with the gaseous phase. The average external force and heat exchange term are \mathbf{F}^k and E_d^k . The mass coupling with the carrier phase is done through $d_f^E = \sum_{k=1}^{N_S} m^k E_2^{(k)}$, where N_S is the total number of sections. A Strang splitting algorithm separates transport in physical space from the evolution in phase space. The numerical schemes involve a very low level of numerical diffusion and are able to deal with singularities and stiffness (de Chaisemartin 2009).

2.2. DNS Configuration and parallel capability

The gas flow is computed with the low Mach dilatable solver available in *Asphodele*. The jet is destabilized with turbulence injection through a Klein's method with 10% of fluctuations (Klein et al. 2003). The coflow is preheated at 750K while fresh gases temperature is injected at 298.15K. The coflow injection velocity is 0.5m/s and the jet injection velocity is 5m/s. We define the Reynolds number based on the geometry by $Re_0 = (U_0 x_0)/\nu_\infty$, where U_0 is the injection velocity, and x_0 is the jet width. A Reynolds number of 1000 is considered in the presented simulations, that corresponds to a jet width $x_0 = 0.315cm$, an injection velocity $U_0 = 5m/s$ for a typical kinematic viscosity $\nu_\infty = 1.6 \times 10^{-5}m^2/s$. Finally, we take $d_0 = x_0/584$, where d_0 is the diameter corresponding to the typical droplet surface S_0 and leads to a Stokes number of 2.7 based on the jet width and injection velocity. The complete domain of the simulation has the dimension $10x_0 \times 4x_0 \times 4x_0$, but due to the symmetries, we only compute one quarter of the whole domain: $10x_0 \times 2x_0 \times 2x_0 = 3.15 cm \times 0.63 cm \times 0.63cm$, with $300 \times 60 \times 60$ grid points for the gas flow. A refined grid of $450 \times 90 \times 90$ grid points is used for the Eulerian spray simulation. Indeed, as a CFL equal to one is used for the MF part, we obtain a time step similar to the one used in the Lagrangian part by taking a lower space discretization (a CFL of 0.4 is used for the gas phase). Concerning the Eulerian phase space discretization, ten sections are used to describe the evaporation process within MF, while only one is used in the non-evaporating case. The number of Lagrangian droplets is determined such as the liquid mass volume fraction at the jet injection is 0.2. The results are presented at time $t = 32 ms$, when the jet has already gone five times across the computational domain.

The gas vorticity field is presented in figure 2. Four planes that will be used to compare the methods are shown: at $x = 5 mm$ near the injection entrance, $x = 10 mm$ and $x = 20 mm$ in the middle of the computational domain and $x = 30 mm$ near the free jet

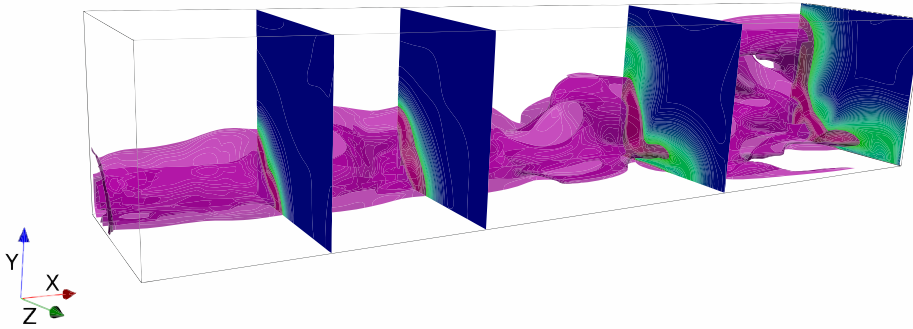


FIGURE 2. Iso-contour of the gas vorticity field at time $t = 32 \text{ ms}$. The four cut planes used for the statistics are represented at $x = 5$, $x = 10$, $x = 20$ and $x = 30 \text{ mm}$ from left to right.

exit. The flow is in a laminar regime at the entrance and becomes turbulent far from it. This allows to validate the Eulerian approach in different regimes.

Monodisperse particles are injected in a jet core with a initial velocity U_0 in the first direction, $\mathbf{u} = (U_0, 0, 0)$. The fact that a monodisperse spray is considered initially underlines the quality of the results. Such an initial Dirac delta function in phase space is one of the most difficult cases to deal with using the MF model for two reasons. First, the discretization in size phase space for the MF leads to a size interval with constant density of the NDF as a function of radius, thus introducing a difference as early as the injection point compared to the Lagrangian injection at a single size. Besides, since polydispersion arises through the coupling of turbulence and evaporation, capturing the proper evaporation dynamics in phase space is similar to solving an advection equation with Dirac delta function initial solution using a finite volume method with coarse discretization. Thus such a case is revealing the intrinsic potential of the MF. Since we aim at validating the Eulerian models through comparisons to a Lagrangian simulation, we restrict ourselves to one-way coupling. We take this Lagrangian simulation as a reference solution for the liquid phase. The two codes have been optimized on parallel architecture, and the Eulerian solver *Muses3d* reaches an efficiency of one up to 512 cores on the Certainty cluster of the Center for Turbulence Research. Results presented here were obtained by using 270 cores, 30 in x-direction and 3 in y- and z-directions. The Euler-Euler simulation with ten sections takes around 12 hours while 9 hours were needed for the Euler-Lagrange simulation to reach the time $t = 32 \text{ ms}$ in the evaporating case. The Euler-Euler description is then a little more time consuming than the Euler-Lagrange; however, as detailed in de Chaisemartin *et al.* (2009), comparing the computational cost of the two solutions is not an easy task. The Lagrangian solution is still not converged and possesses a high level of noise. Reducing the noise in the Lagrangian simulation would require to increase the number of samples, whereas, as we will refine the grid, the parallel ability of the Eulerian simulation will improve compared to the Lagrangian one. Besides, two-way coupling would require additional computational cost in the Lagrangian formalism compared to the Eulerian one.

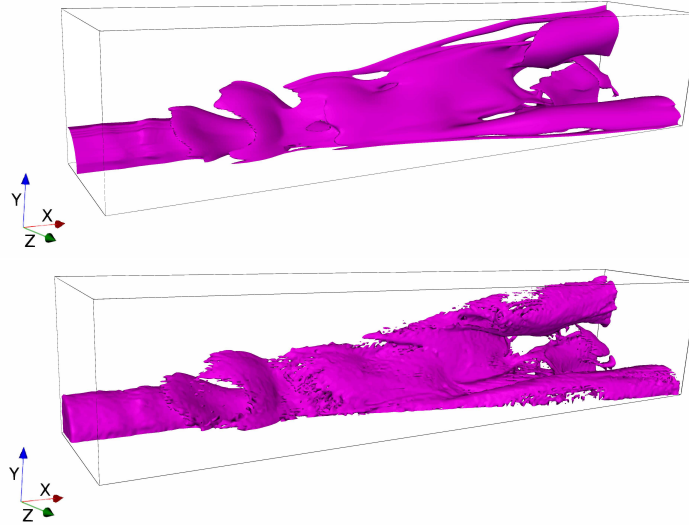


FIGURE 3. Qualitative comparison of the liquid mass obtained with the MF model (top) and the Lagrangian one (bottom) at time $t = 32 \text{ ms}$. The liquid phase stoichiometric iso-contour 0.0625 is represented.

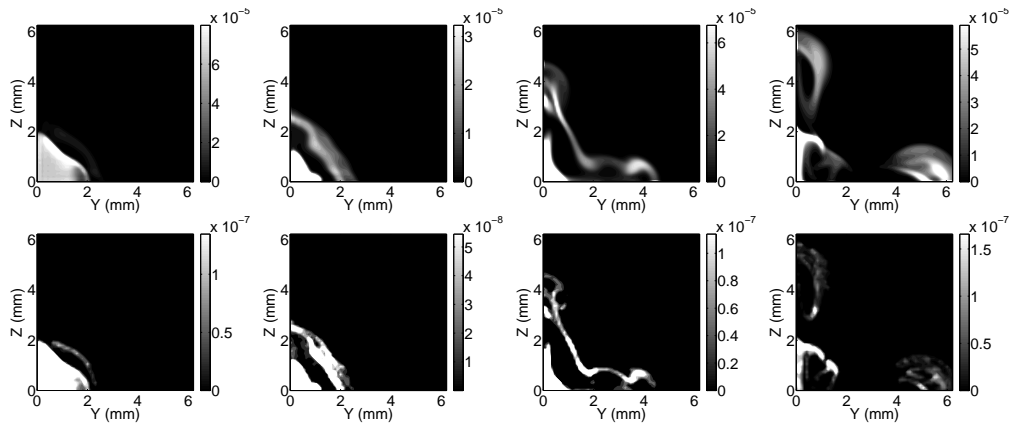


FIGURE 4. Comparison of the liquid mass obtained with the MF model (top) and the Lagrangian one (bottom) at time $t = 32 \text{ ms}$ for $x = 5 \text{ mm}$, $x = 10 \text{ mm}$, $x = 20 \text{ mm}$ and $x = 30 \text{ mm}$ from left to right.

3. Results and discussion

The objective is to carry out qualitative but also quantitative comparisons between both Lagrangian and Eulerian formulations. Because of its intrinsic properties, the results from the Lagrangian solver are considered as a reference, even if we have not yet reached a converged solution in terms of noise. The MF solver is able to capture the spray dispersion and segregation as well as a correct evaluation of the fuel vapor topology.

3.1. Spray dispersion and segregation

For the non-evaporating case we use only one section for the MF monodispersed spray simulation. We have about 1 500 000 Lagrangian particles in the computational domain at

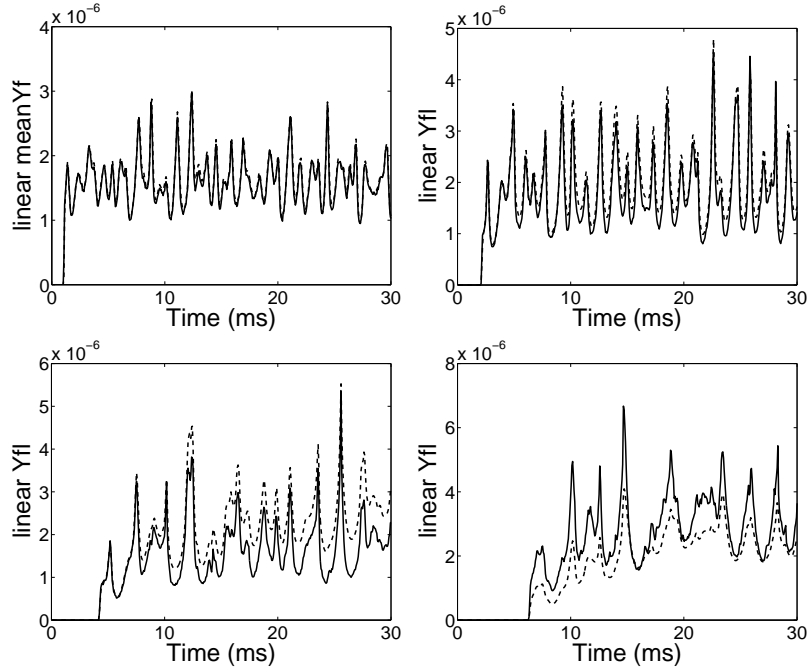


FIGURE 5. Mean mass time evolution along the flow in the sectional plane $x = 5 \text{ mm}$ (top left), $x = 10 \text{ mm}$ (top right), $x = 20 \text{ mm}$ (bottom left) and $x = 30 \text{ mm}$ (bottom right). The Lagrangian description is represented by a continuous line and the MF is represented by a dashed line.

the considered time $t = 32 \text{ ms}$. In figure 3 we present two snapshots of the Eulerian (top) and Lagrangian (bottom) iso-contour of the liquid mass volume fraction. The iso-contour value 0.0625 has been chosen since it corresponds to the n-heptane stoichiometry. This first qualitative comparison shows a very good agreement between the two approaches all along the jet. Due to the noise induced by the Lagrangian formalism, the iso-contour of droplets density shows some ligaments, which are not visible with the MF method. We also provide in figure 4 comparisons between MF (top) and the reference Lagrangian description (bottom) in the four planes all along the flow at $x = 5 \text{ mm}$, $x = 10 \text{ mm}$, $x = 20 \text{ mm}$ and $x = 30 \text{ mm}$ from left to right. These detailed comparisons show a very good agreement since the jet core is very well reproduced as well as external recirculations between both approaches. Finally we complete this study with a quantitative comparison of the time evolution of the linear liquid mass in figure 5. In the same four planes along the x-direction, we plot the evolution of the Lagrangian (solid line) versus the Eulerian (symbols) mean liquid mass in the planes per unit of x length. The very good agreement all along the flow between MF and the Lagrangian description assess the capacity of the MF method to simulate such a complex flow with a monodisperse non-evaporating spray. The MF method is thus able to simulate the dynamics of a spray where droplet crossings are limited, the model remaining therefore in its validity domain.

3.2. Spray evaporation

The free jet is also assessed with an evaporating spray. An IAT law is considered, the temperature T has been utilized through the following expression of the mass transfer

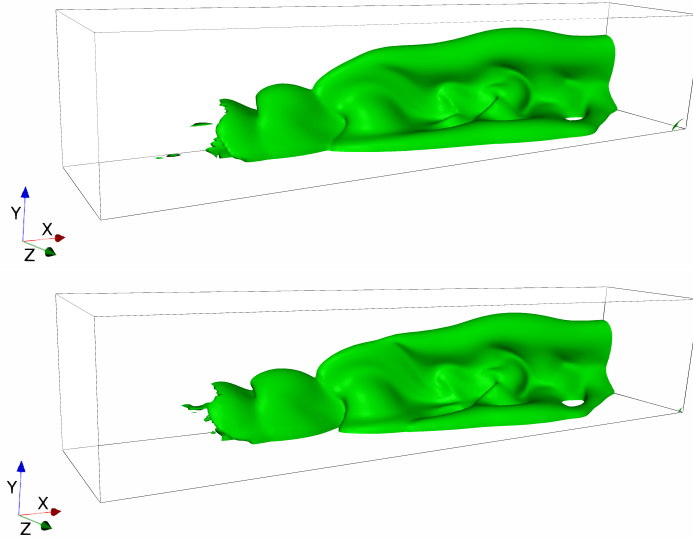


FIGURE 6. Qualitative comparison of the fuel mass fraction obtained with the MF model (top) and the Lagrangian one (bottom) at time $t = 32 \text{ ms}$. The stoichiometric iso-contour 0.0625 is represented.

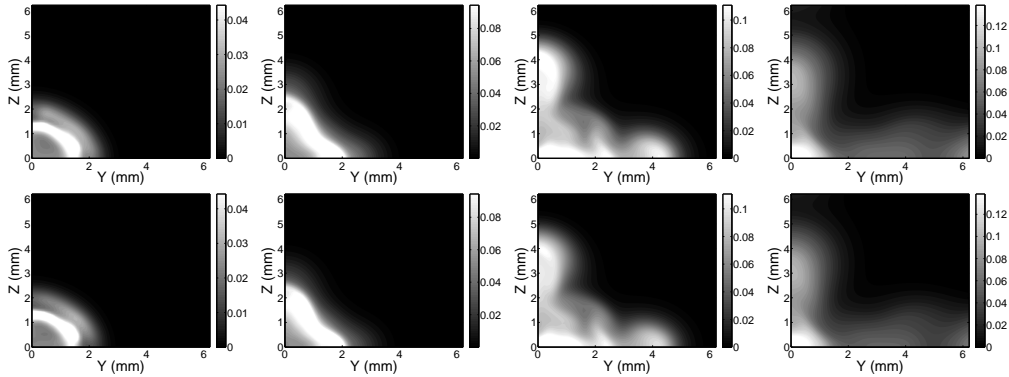


FIGURE 7. Comparison of the fuel mass fraction obtained with the MF model (top) and the Lagrangian one (bottom) at time $t = 32 \text{ ms}$ for $x = 5 \text{ mm}$, $x = 10 \text{ mm}$, $x = 20 \text{ mm}$ and $x = 30 \text{ mm}$ from left to right.

number

$$B = \frac{T - T_0}{T_b - T_0} \left(\exp \left(\frac{A a_0^2}{\tau_v} \right) - 1 \right), \quad (3.1)$$

where A is a constant depending on liquid and gas properties (Reveillon & Demoulin 2007) and $T_b = T_a(Y_b = 1)$ the burnt gases temperature. B is introduced in the expression of the evaporation rate through the evaporation time $\beta_k^{(a)}$ defined by $\beta_k^{(a)} = A a_k^2 / \ln(1 + B)$. In order to describe correctly the evaporation process, the MF simulations are performed with ten sections. The liquid mass volume fraction is still equal to 0.2 as in the previous non-evaporating case but due to evaporation process, about 700 000 Lagrangian particles are present in the domain at the considered time $t = 32 \text{ ms}$. We have compared the size conditioned dynamics of various droplet size intervals and ob-

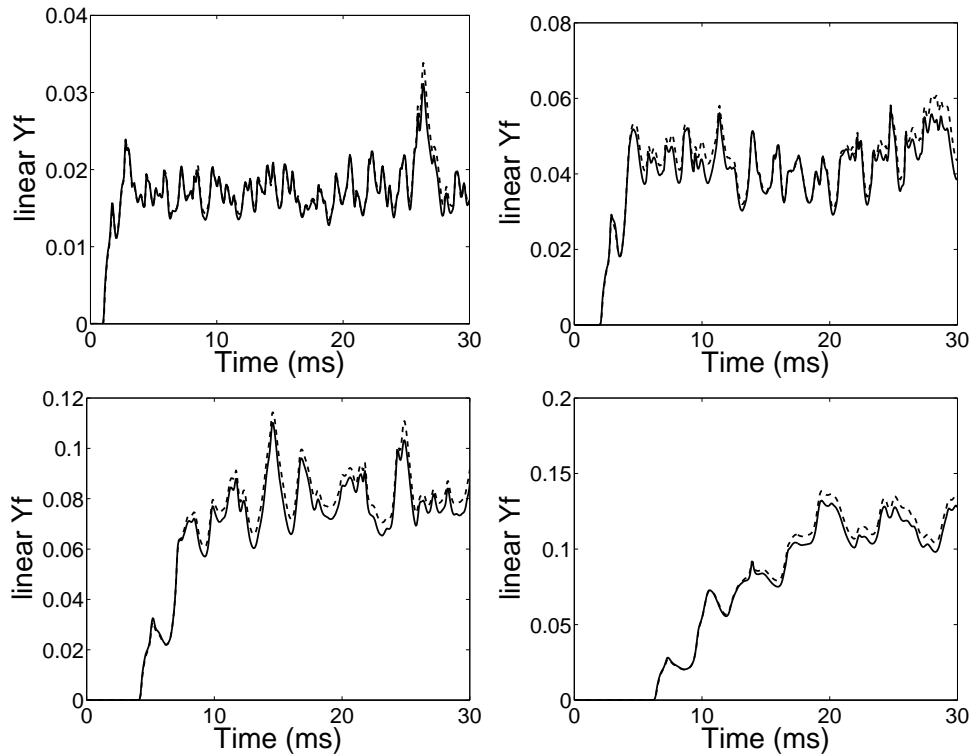


FIGURE 8. Mean fuel mass fraction time evolution along the flow in the sectional planes $x = 5 \text{ mm}$ (top left), $x = 10 \text{ mm}$ (top right), $x = 20 \text{ mm}$ (bottom left) and $x = 30 \text{ mm}$ (bottom right). The Lagrangian description is represented by a continuous line and the MF is represented by symbols.

tained results similar to what has been shown in the non-evaporating case in figure 3. As already described in previous studies, MF is able to capture size-conditioned dynamics of droplets of various sizes. It is then essential to evaluate the ability of the Eulerian model to predict the evaporation process as a whole. Because our interest is in combustion applications, a key quantity is the gaseous fuel mass fraction. We thus present comparisons between this gaseous fuel mass fraction, obtained from the Lagrangian and MF descriptions of the spray. Once again the gaseous flow field is the same in both cases. In figure 6, we plot the iso-contour 0.0625 of the fuel mass fraction obtained thanks to MF model (top) and the Lagrangian model (bottom) at time $t = 32 \text{ ms}$. One can see the very good agreement of both descriptions for spray evaporation. This is a promising result for our ongoing work on combustion simulation since this stoichiometric iso-contour represents the potential location for a propagating flame. In the four planes defined along the x -axis, we present in figure 7 a Eulerian (top) and Lagrangian (bottom) comparison of the fuel mass fraction at time $t = 32 \text{ ms}$. After five domain crossings, the level of comparison is excellent. Finally, we provide the time evolution of the linear fuel mass fraction averaged in the previous planes per unit x length in figure 8. The Lagrangian results are plotted using a solid line while Eulerian ones are presented using symbols. This comparison underlines the efficiency of the MF in describing polydisperse evaporating sprays. Such a level of comparison allows us to consider the reacting case as a natural perspective of the present work.

Acknowledgments

The authors wish to thank the Center for Turbulence Research at Stanford University for its hospitality, financial and technical support. This work was granted access to the HPC resources of IDRIS-CINES under the allocations 2012-x2012026172 (M. Massot) by GENCI. The support of the France-Stanford Center for Interdisciplinary Studies through a collaborative project grant (PIs: P. Moin / M. Massot) is also gratefully acknowledged.

REFERENCES

- DE CHAISEMARTIN, S. 2009 Polydisperse evaporating spray turbulent dispersion: Eulerian model and numerical simulation. PhD thesis, Ecole Centrale Paris.
- DE CHAISEMARTIN, S., FRÉRET, L., KAH, D., LAURENT, F., FOX, R., REVEILLON, J. & MASSOT, M. 2009 Eulerian models for turbulent spray combustion with polydispersity and droplet crossing. *Comptes Rendus Mécanique* **337**, 438–448.
- DOISNEAU, F., THOMINE, O., LAURENT, F., VIÉ, A., DUPAYS, J. & MASSOT, M. 2012 Eulerian modeling and simulation of small scale trajectory crossings and coalescence for moderate-stokes-number spray flows. In *Proceedings of the summer program 2012, Center for Turbulence Research, Stanford University*, pp. 1–10.
- FRÉRET, L., THOMINE, O., LAURENT, F., REVEILLON, J. & MASSOT, M. 2012 On the ability of the Eulerian multi-fluid model to predict preferential segregation and flame dynamics in polydisperse evaporating sprays. *Combustion and Flame (submitted)*.
- FRÉRET, L., THOMINE, O., REVEILLON, J., DE CHAISEMARTIN, S., LAURENT, F. & MASSOT, M. 2010 On the role of preferential segregation in flame dynamics in polydisperse evaporating sprays. In *Proceedings of the summer program 2010, Center for Turbulence Research, Stanford University*.
- GARCIA, M. 2009 Développement et validation du formalisme euler-lagrange dans un solveur parallèle non-structuré pour la simulation aux grandes échelles. PhD thesis, Institut National Polytechnique de Toulouse.
- KAH, D., LAURENT, F., FRÉRET, L., DE CHAISEMARTIN, S., FOX, R., REVEILLON, J. & MASSOT, M. 2010 Eulerian quadrature-based moment models for polydisperse evaporating sprays. *Flow, Turbulence and Combustion* **85** (3-4), 649–676.
- KLEIN, M., SADIKI, A. & JANICKA, J. 2003 A digital filter based generation of inflow data for spatially developing direct numerical or large eddy simulations. *J. Comput. Phys.* **186**, 652–665.
- LAURENT, F. & MASSOT, M. 2001 Multi-fluid modeling of laminar poly-dispersed spray flames: origin, assumptions and comparison of the sectional and sampling methods. *Combustion Theory and Modelling* **5**, 537–572.
- MASSOT, M., DE CHAISEMARTIN, S., FRÉRET, L., KAH, D. & LAURENT, F. 2009 Eulerian multi-fluid models: modeling and numerical methods. In *Modelling and Computation of Nanoparticles in Fluid Flows*, pp. 1–86. Lectures of the von Karman Institute. NATO RTO AVT 169.
- THOMINE, O. 2011 Développement de méthodes multi-échelles pour la simulation numérique des écoulements réactifs diphasiques. PhD thesis, University of Rouen.
- VIÉ, A., MASI, E., SIMONIN, O. & MASSOT, M. 2012 On the direct numerical simulation of moderate-stokes-number turbulente particulate flows using algebraic-closure-based and kinetic-based moment methods. In *Proceedings of the summer program 2012, Center for Turbulence Research, Stanford University*, pp. 1–10.